Iranian Journal of Medical Physics

ijmp.mums.ac.ir

Dosimetric and Biological Outcomes of Gamma Knife Radiosurgery and Volumetric Modulated Arc Therapy

Gad Elbaz[1*], Ibrahim M. Hassan[2], Khairy.T. Ereiba[2], Ehab Attalla[3]

1. Gamma knife Damietta Center, Department of Neurosurgery, faculty of medicine, Damietta Al-Azhar university Hospital. Cairo, Egypt.
2. Physics Department, Faculty of Science, Al-Azhar University, Cairo, Egypt.
3. National Cancer Institute, Cairo University, Giza, Egypt.

ARTICLE INFO

Article type:
Original Paper

Article history:
Received: Jun 16, 2025
Accepted: Dec 01, 2025

Keywords:
Second Cancer risk
GKR
VMAT
TCP
NTCP
Meningioma

ABSTRACT

Introduction: This research aimed to evaluate the radiation-induced secondary cancer risks in normal tissues following Gamma Knife Radiosurgery (GKR) compared with the Volumetric-Modulated Arc Therapy (VMAT).

Material and Methods: Eleven patients with meningioma (2 males, 9 females; median age 30 years) were analyzed. For each case, Gamma Knife radiosurgery (GKR) and volumetric modulated arc therapy (VMAT) plans were created and compared using dosimetric-metrics and radiobiological modeling. The Organ Equivalent Dose (OED) was estimated using linear, linear-exponential, and plateau dose–response models, and the Excess Absolute Risk (EAR) was calculated for organs at risk to estimate secondary cancer risk.

Results: Dose coverage, conformity, and homogeneity in the Planning Target Volume (PTV) improved significantly ('p'< 0.05) with GKR and VMAT. Higher OED was observed in the optic nerve due to proximity to the target. While the EAR of the optic nerve increased by 11.23%, 13.17%, and 14.86% in GK compared to VMAT for the linear, plateau, as well as linear-exponential models, respectively, in GK plans compared to VMAT, the EAR for the brain stem increased by 54.4%, 17.14%, and 30% in VMAT. GKR had a considerably greater Tumor Control Probability (TCP) (95.76%±2.86) than VMAT (84.29%± 2.27, 'p'= 2.8×10^{-6}).

Conclusion: GKR provided better PTV dose coverage and conformity, whereas VMAT achieved superior dose homogeneity. According to EAR, VMAT had a greater second cancer risk than GK. For young patients, advanced radiotherapy techniques should be evaluated in consideration of dosimetric, radiobiological, and secondary cancer risks.

►*Please cite this article as:*
Elbaz G, Hassan IM, Ereiba Kh, Attalla E. Dosimetric and Biological Outcomes of Gamma Knife Radiosurgery and Volumetric Modulated Arc Therapy. Iran J Med Phys 2025; 22 (6): 377-388. 10.22038/ijmp.2025.88946.2568.

Introduction

Meningiomas represent the most common primary intracranial neoplasm of the central nervous system (CNS)[1]. Although frequently characterized as biologically indolent, their dural origin and proximity to critical neurological structures may produce clinically relevant morbidity arising from mass effect or functional compromise. Surgical resection remains the initial therapeutic modality, while adjuvant fractionated radiotherapy (RT) or stereotactic radiosurgery (SRS) is considered based on the residual disease and risk of recurrence. Selection of the optimal radiation approach should be individualized by integrating patient-specific clinical variables, expected survival, pathologic and molecular classification, lesion geometry, and the feasibility of achieving adequate dosimetric coverage while maintaining organ-at-risk (OAR) constraints [2].

The use of fractionated or single fraction stereotactic radiotherapy to treat meningiomas is still in its infancy. For limited-volume tumors, stereotactic radiotherapy, such as Volumetric Modulated Arc Therapy (VMAT), has been used instead of external-beam radiation using the linear accelerator, Leksell Gamma Knife, or Cyberknife [3].

The Leksell Gamma Knife utilizes sealed radioactive sources in conjunction with a stereotactic delivery system to deliver highly conformal, high-dose irradiation to the intended intracranial target while maintaining a steep dose fall-off to adjacent healthy structures. This platform is widely validated for treating neoplastic, vascular, and select functional intracranial pathologies. The principal advantage of stereotactic localization lies in its ability to restrict radiation exposure to surrounding organs at risk (OARs). Consequently, comparative evaluation of planning strategies is warranted, particularly with respect to long-term radiobiological implications such as second cancer risk (SCR). Although stereotactic systems significantly limit peripheral dose, ionizing radiation exposure, both within the primary

*Corresponding Author: Tel: +20 101 618 1283; +201147280179; Email: elbazgedo@gmail.com

treatment volume and throughout out-of-field scatter, remains a recognized contributor to secondary malignancy development in irradiated patients [4–5].

Previous comparative analyses in patients with nasopharyngeal carcinoma have demonstrated that second cancer risks estimated using Organ Equivalent Dose (OED) models were generally similar between VMAT and intensity-modulated radiotherapy (IMRT). Nonetheless, a slightly elevated projected risk was reported for structures such as the oral cavity and mandible when VMAT plans were employed [6].

This study aims to compare the radiobiological performance of GK and VMAT treatment plans for meningioma by analyzing modeled Tumor Control Probability (TCP) and Normal Tissue Complication Probability (NTCP) for critical structures, including the brainstem and optic nerve, along with key dosimetric parameters derived from each technique.

In addition, the OED framework, using three dose–response models (linear, linear-exponential, and plateau), is applied to quantify and compare the projected SCR for the brainstem and optic nerve following GK and VMAT planning.

Materials and Methods

Patients and Materials

Patient Cohort and Pathological Characteristics

A total of eleven patients with intracranial meningioma underwent GK treatment between March 2020 and March 2024. The cohort consisted of nine females and two males, with a median age of 30 years (range, 20–38 years). Tumor locations were heterogeneous, including Petro-clival (n=3), cavernous (n=2), Sphenoid wing (n=1), petrous apex(n=2), Cerebellopontine Angle (CPA) (n=2), deep Parietal (n=1). Diagnosis was established based on characteristic neuroimaging findings on brain CT and MRI. Lesions appeared slightly hyperdense on non-contrast CT and demonstrated strong, homogeneous post-contrast enhancement with a typical dural tail, occasionally associated with adjacent hyperostosis. MRI showed consistent post-contrast enhancement and lesions that were primarily isointense to cortical gray matter on T1-weighted sequences. Restricted diffusion was seen on DWI/ADC, and T2-weighted images displayed iso- to hyperintensity. All cases were assessed by a multidisciplinary neuro-oncology board to establish the best therapeutic approach, and each patient provided written informed consent following comprehensive counseling about procedure stages, projected benefits, and potential risks.

Volumetric modulated arc therapy (VMAT)

VMAT is an advanced external beam technique that delivers highly conformal dose distributions to the target while minimizing exposure to surrounding normal tissue through one or multiple continuous arcs. Similar to IMRT, dose modulation is achieved using a multileaf collimator capable of dynamic shaping during beam delivery. In dual-arc VMAT planning, two full arcs are typically employed for centrally located lesions, whereas peripheral targets may utilize two additional partial arcs to optimize coverage and OAR sparing [7].

Radiation was delivered to the target from multiple beam angles, with continuous dynamic motion of the multileaf collimator used to modulate the intensity and conform the dose to the three-dimensional shape of the tumor. This approach enabled highly selective dose deposition while limiting exposure to adjacent normal tissues [8]. A further advantage was the reduction in overall treatment delivery time resulting from continuous arc modulation. In the current study, all VMAT plans were generated and delivered using a VersaHD photon treatment system in Stockholm, Sweden. Planning parameters included 220 segments and a mean requirement of approximately 12,000 monitor units per fraction. Dose computation was performed using the XVMC v1.6 algorithm, and treatments were executed with 6.0-MV flattening filter-free (FFF) photon beams. Removal of the flattening filter from the accelerator head enabled two- to three-fold higher dose rates than conventional flattened beams, thereby improving delivery efficiency and minimizing intrafraction time.

Leksell Gamma Plan (LGP)

Stereotactic GK Perfexion® radiosurgery, used for non-invasive management of intracranial lesions, was simulated and planned using Leksell Gamma Plan (LGP) version 10.1. The LGP platform operated in a step-and-shoot delivery mode, and planning was conducted using the ball-packing technique, in which multiple spherical high-dose volumes (“shots”) of varying collimator sizes were arranged to fill the tumor volume conformally. The contouring of each meningioma was modified using a range of collimator sizes, including 4mm, 8mm, and 16mm, in addition to various filling sector techniques to fit and avoid the OAR. Tomographic and projection images indicate that it employs 192 fixed Cobalt-60 sources, thereby reducing the potential for inaccuracy due to stationary sources and ensuring the maximum level of precision throughout treatment [9].

Treatment Planning (Monaco 6.1.2.0)

VMAT plans were optimized in Monaco (version 6.1.2.0, research build, executed on dual Quadro GV100 32-GB NVIDIA GPUs) using the original ATS plan template, which included predefined cost functions and parameter constraints. The Planning Target Volume (PTV) was generated through an isotropic expansion of the Clinical Target Volume (CTV). MRI datasets and corresponding structure sets from daily treatments were imported into the Treatment Planning System(TPS) via DICOM-RT protocols. Target volumes and OARs were contoured on the imported MRI according to Radiation Therapy Oncology Group (RTOG) guidelines, and electron density overrides were applied to structures

exhibiting potential overlap across plans. A prescribed single-fraction dose of 12 Gy was assigned to cover the Gross Tumor Volume (GTV) fully. OARs of interest included the brainstem, ipsilateral optic nerve, infundibulum, and pituitary gland.

MATLAB R2016a

MATLAB® Programming: A custom MATLAB® application, designated *PROGTCP*, was developed to extract volumetric and dose-percentage data from Dose Volume Histogram (DVH). The program required users to input the relevant radiobiological parameters, including the α/β ratio for the selected organ, the slope of the dose-response curve at 50%, the tolerance dose at 50%, and the *m* parameter that defines the steepness of the complication-probability curve. Once these inputs were provided, *PROGTCP* automatically generated calculated TCP and NTCP values [10].

Statistical Analysis

SPSS version 20 (IBM; IL) was utilized for data analysis and statistics. The significance of the differences was determined using a paired sample t-test. The differences between treatment plan techniques were statistically significant if the 'p'-value of < 0.05 was obtained from an independent Samples t-test. All descriptive data for Gamma Knife treatment plans are shown in Table 3.

Methods

Dosimetric and Radiobiological Plan Evaluation

The OED and EAR calculations:

SCR following radiotherapy was expressed as EAR, reported per 10,000 persons per year per Gy. EAR represented the absolute increase in cancer incidence among individuals exposed to therapeutic radiation compared with those receiving only background exposure. EAR values were derived using Equation (1) as described in the following referenced methodology [11].

$$EAR=EAR_0\times OED \quad (1)$$

EAR_0 denoted the initial slope of the dose–response curve in the low-dose region and incorporated population-dependent variables, including age at exposure (age_x), sex (s), and attained age (age_a) [27]. The EAR for secondary malignancy development in each evaluated organ was subsequently computed using Equation (2) as outlined below*:*

$$EAR=OED\ \beta' \exp\left[\gamma_e\,(agex-30)+\gamma_a \ln(agea/70)\right] \quad (2)$$

In this model, β′ represented the initial slope of the dose–response relationship for radiation-induced second malignancies, whereas γ_e and γ_a denoted the modifying factors for age at exposure and attained age, respectively. All numerical inputs used for EAR estimation were summarized in Table 1. OED values for the evaluated OARs were calculated from differential DVH data using three dose–response formulations: linear, linear-exponential, and plateau models [12].

Table 1. OED and EAR Calculation Parameters and Source of Dosimetric Data(Schneider et al., 2011)[13].

Organ	$B_{inatial}$	γ_e	γa	Source of dose
Brain	0.7	-0.024	2.38	DVH

In this study, the patients' ages at exposure (age_x) ranged from 20 to 38 years, and the attained age was set at 70 years for all SCR estimations. In the linear dose–response model, it was assumed that the induction probability increased proportionally with the absorbed dose to a given organ. The linear OED for an organ *T* (OED^T, linear) was calculated using Equation (3) as shown below.

$$OED_T=1/V_T\sum_i DVH(Di)Di \quad (3)$$

In this formulation, $DVH(D_i)$ referred to the fractional organ volume receiving dose level D_i, and the summation was performed over all voxels comprising organ *T*, with a total volume denoted as V^T.

The linear–exponential formulation accounted for the assumption that radiation-induced cell lethality increased exponentially with absorbed dose, thereby reducing the likelihood of malignant transformation by eliminating mutated cells. The corresponding OED for this dose–response model was calculated using Equation (4) as follows:

$$OED_T=1/V_T\sum_i DVH(Di)Di\ e^{-\alpha Di} \quad (4)$$

Where $\alpha = 0.044\ Gy^{-1}$ [14].

The plateau model assumed that the dose–response relationship increased linearly at lower dose levels until reaching a saturation point, beyond which additional dose did not further elevate risk due to effective tumor-cell sterilization and comprehensive repair capacity within normal tissues under fractionated exposure conditions. The corresponding OED for this model ($OED_{plateau}$) was computed using Equation (5) as outlined*:*

$$OED_T=1/V_T\sum_i DVH(Di)(1-e^{-\delta Di})/\delta \quad (5)$$

The parameters α and δ were derived from a combined statistical fit to epidemiological data obtained from the Japanese atomic-bomb survivor cohort and patients treated for Hodgkin disease [14].

Radiobiological Evaluation Models

The EUD-based mathematical framework was considered both simple and flexible, as it relied primarily on two core equations and could be applied uniformly for estimating both TCP and NTCP, as defined in Equations (6) and (7)[15].

$$TCP=\frac{1}{1+(\frac{TCD50}{EUD})^{4\gamma 50}} \quad (6)$$

$$NTCP=\frac{1}{1+(\frac{TD50}{EUD})^{4\gamma 50}} \quad (7)$$

In this formulation, TCD_{50} represents the dose required to achieve local control in 50% of tumors under conditions of homogeneous irradiation, whereas TD_{50} denotes the dose associated with a 50% probability of developing clinically

significant toxicity within a specified evaluation period, based on established tolerance data. The parameter γ_{50} described the steepness of the corresponding dose–response curve. The EUD was then computed using Equation (8):

$$EUD = (\sum v_i D_i^a)^{1/a} \quad (8)$$

In this model, V_i referred to the fractional subvolume of an organ receiving dose level D_i, while the parameter a described the tissue-specific dose–response sensitivity. In the present study, the values of aAlong with the parameters TD_{50}, γ_{50}, and α/β for late-responding tissues (evaluated at 5 years), which were adopted as reported in the literature and summarized in Table 2 [16–17].

Abbreviations: α/β=alpha beta ratio; TD_{50}= tolerance dose for 50% of complication; γ_{50} is a unitless model parameter that is specific to the normal structure or tumor.

In order to assess the TCP-values using physical indices from DVH, the values for TCD50 and $\gamma 5_0$ for adjuvant radiation and curative goal were examined. These MATLAB-written equations are used to examine each patient's DVH using a particular application. Import this data into MATLAB as EUDMODEL (DVH), where DVH might be a two-column matrix that resembles the cumulative dose-volume histogram rather than a percentage. Increasing absolute dosage is shown by the first column, and matching absolute volume is represented by the second. There should be at least two rows in the matrix, and each column should have the same length [18].

Dose-metrical Parameters

According to ICRU Report 83[19], comparative plan evaluation between the two techniques was performed using cumulative and differential DVHs generated from the LGP and VMAT dose distributions. For PTV assessment, the parameters analyzed included the mean dose (D_{mean}) and the percentage target volume receiving 100% of the prescribed dose (V_{100}).

Homogeneity Index (HI)

The HI was applied as an objective metric to quantify dose uniformity within the target. It was defined as the ratio between the maximum and minimum dose delivered to the target volume, where lower values denoted a more homogeneous distribution, as expressed in Equation (9).

$$HI = D2\% - D98\% \quad (9)$$

Conformity Index (CI)

CI was defined as the ratio between the volume encompassed by the prescribed isodose (V_{PD}) and the portion of the PTV receiving at least the prescribed dose (PTVPD), as described in Equation (10)[7].

$$CI = VPD/PTV_{PD} \quad (10)$$

For intracranial meningiomas, the optimal dose-metrical parameters were CIn < 2.0 and HIn ≤ 2.0 [7-4].

Treatment protocol

This study was structured to enable detailed DVH analysis. All included cases involved benign intracranial meningiomas of variable volumes located adjacent to critical OARs. Patients were treated using single-session stereotactic radiosurgery planned on the Leksell Gamma Plan system, with a prescribed marginal dose of 12 Gy delivered at the 50% isodose line. A representative gamma knife dose distribution for a benign intracranial meningioma is displayed in Figure 1:

Table 2. Radiobiological parameters used to calculate NTCP and TCP

Structures		a	γ_{50}	TD_{50} / TCD50 (Gy)	α/β	References
Tumor	Meningioma	-8	2.5	11	4	[5]
Organs at risk (QAR)	Optic nerve	25	3	10	4	Niemierko, A. [16]
	Brain Stem	7	3	15	4	Elbaz, G [4]

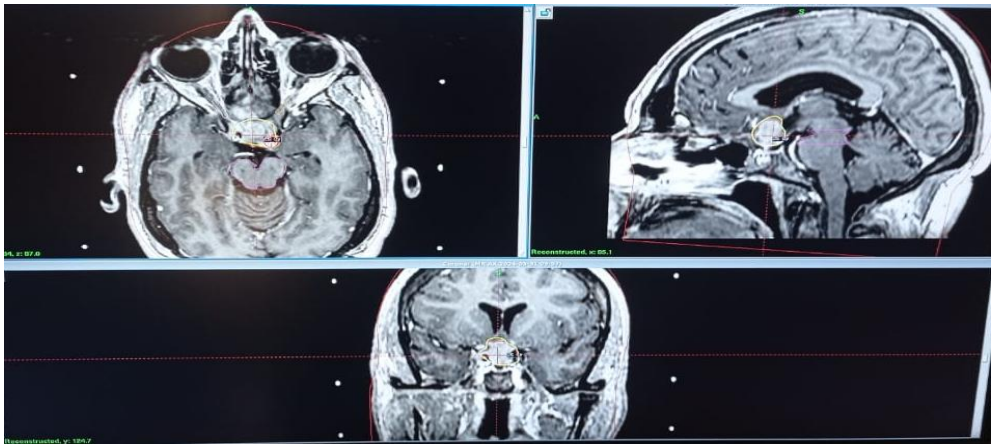

Figure 1. Dose Distribution in Benign Intracranial Meningioma treatment using Gamma knife technique

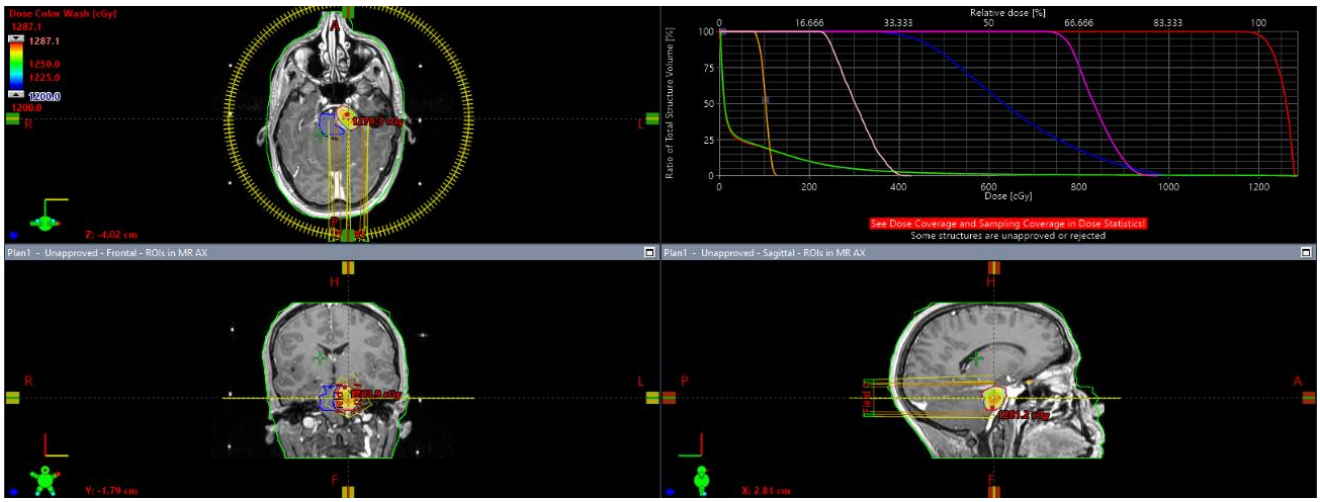

Figure 2. Snapshots of treatment plan and dose distribution in intracranial meningioma using VMAT technique.

In benign intracranial meningioma radiosurgery, the principal OARs include the brainstem and the bilateral optic nerves [28]. Standard planning parameters were applied in the Leksell Gamma Plan software after defining the prescription dose and prescription isodose line. Following finalization of the GK plans, all cases were exported and re-evaluated using a separate treatment planning workflow based on VMAT for the same target volumes. Consequently, two comparative plans (GK and VMAT) were generated for each patient.

Different treatment plans can produce dose distributions with similar global metrics, such as mean dose, yet yield DVHs of markedly different shapes. Corresponding MRI-based localization and VMAT-derived PIV (Prescription Isodose Volume) visualization for the investigated tumor volume are demonstrated in Figure 2. In such scenarios, plan selection cannot rely solely on conventional physical dose parameters, and clinicians may need to interpret dose-volume characteristics qualitatively. Therefore, radiobiological modeling provides an objective framework for ranking treatment plans through the quantitative estimation of second-cancer-related metrics, including OED and EAR, along with TCP and NTCP, using models that incorporate tissue-specific dose-volume behavior and available clinical data [20–21].

Results

Radiobiological Assessment of Gamma Knife Treatment Plans

All calculated EUD-based radiobiological outputs for both planning techniques are summarized in Tables 4 and 5 (a and b). Table 4 reports the TCP values, whereas Table 5 presents NTCP results, with part (a) representing the brainstem and part (b) representing the optic nerve.

Table 3. Patient treatment plans and their information for Gamma Knife treatment technique.

Patient group	Gander	Age[Y]	Diagnosis	Target Volume TV(cc)	Prescription Isodose Volume [PIV] (cc)	Max dose [MD] (Gy)
1	Male	30	RT middle sphenoid cavernous sinus Meningioma	4.2	4.1	24
2	Female	20	RT Petrous Meningioma	1.52	1.49	24
3	Male	24	RT clival small meningioma	0.61	0.6	24
4	Female	26	petro-clival-meningioma	7.47	7.14	24.3
5	Female	27	Residual LT deep Parietal meningioma	5.18	5.11	24.1
6	Female	31	RT Petrous & cavernous sinus meningioma	7.2	6.7	24.2
7	Female	36	CPA Meningioma	5	4.92	24.4
8	Male	37	CPA Meningioma	7.7	7.27	24.5
9	Female	38	Cavernous & Petro clival meningioma	13.6	11.9	24.4
10	Female	38	Cavernous & Petro clival meningioma	9.88	9.65	27
11	Female	38	Meningioma	6.37	6.29	24.3

Table 4. EUD and TCP for Meningioma in GK and VMAT Plans

No of cases	EUD (Gy)		TCP(%)	
	GK	VMAT	GK	VMAT
1	16.2	13.2	97.91%	85.84%
2	15.9	13.4	97.61%	87.47%
3	16.4	12.7	98.19%	80.61%
4	14.3	12.9	93.16%	83.37%
5	16.2	13.2	97.94%	84.85%
6	13.9	12.4	91.27%	82.70%
7	15.5	13	96.90%	85.25%
8	14.3	13.2	93.22%	85.98%
9	10.9	12.5	91.40%	80.68%
10	15.9	13.4	97.57%	86.50%
11	16.4	12.7	98.23%	83.98%
Average	15.1	12.96	95.76%	84.29%
SD	1.7	0.35	2.86	2.27
'p'-value	0.001		2.8×10^{-6}	

Table 5a. EUD and NTCP for Brain Stem in GK and VMAT Plans.

Brain Stem				
No of cases	EUD (Gy)		NTCP(%)	
	GK	VMAT	GK	VMAT
1	1.8	3.7	0.00001%	0.0006%
2	3.6	5.1	0.000034%	0.00021%
3	4.12	4.75	0.00002%	0.0001%
4	4.02	5.91	0.00001%	0.0013%
5	3.92	6.01	0.00001%	0.0012%
6	3.5	5.1	0.00002%	0.0003%
7	2.94	3.89	0.00002%	0.0003%
8	4.6	5.35	0.00007%	0.0004%
9	4.14	5.05	0.00002%	0.009%
10	3.5	5.1	0.00003%	0.0003%
11	5.14	7.04	0.0002%	0.08%
Average	3.75	5.18	0.00005%	0.0085%
SD	0.87	0.94	0.00008	0.023
'p'-value	0.004		0.0001	

Table 5b. EUD and NTCP for Optic Nerve in GK and VMAT Plans.

Optic Nerve				
No of cases	EUD (GY)		NTCP(%)	
	GK	VMAT	GK	VMAT
1	3.96	7.17	0.002%	1.83%
2	0.37	0.75	0.0003%	0.003%
4	0.4	1.1	0.0002%	0.002%
6	2.9	4.8	0.003%	0.01%
7	2.6	4.2	0.002%	0.01%
8	0.6	0.85	0.0001%	0.0002%
9	6.7	8.5	1.1%	1.51%
10	2.5	6.2	0.0007%	1.30%
Average	2.5	4.2	0.13%	0.58%
SD	2.15	3	0.39	0.31
'p'-value	0.141		0.045	

Abbreviations: EUD= Equivalent Uniform Dose; NTCP= Normal Tissue Complication Probability; SD= Standard Deviation.

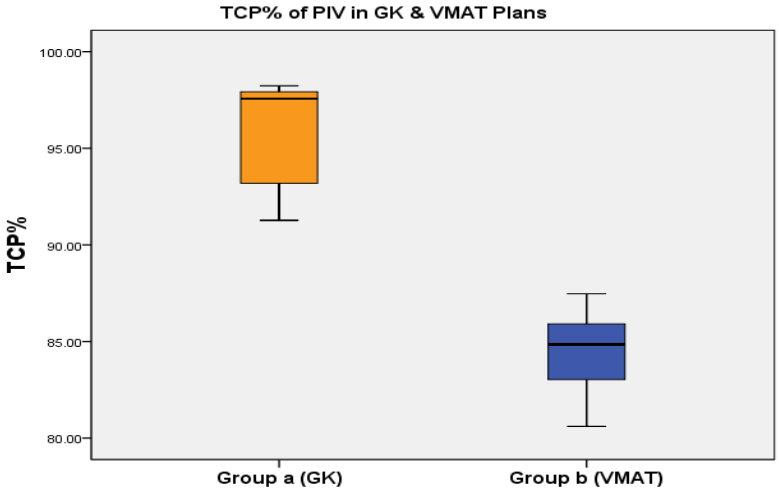

Mean± SD of group (a) 95.76%±2.86
Mean± SD of group (b) 84.29%± 2.27 ('p'= 2.8×10^{-6}, Mann-Whitney test)
Figure 3. Reveals the effect of the value of TCP% of PIV for both techniques (GK) and (VMAT) on Meningioma, respectively.

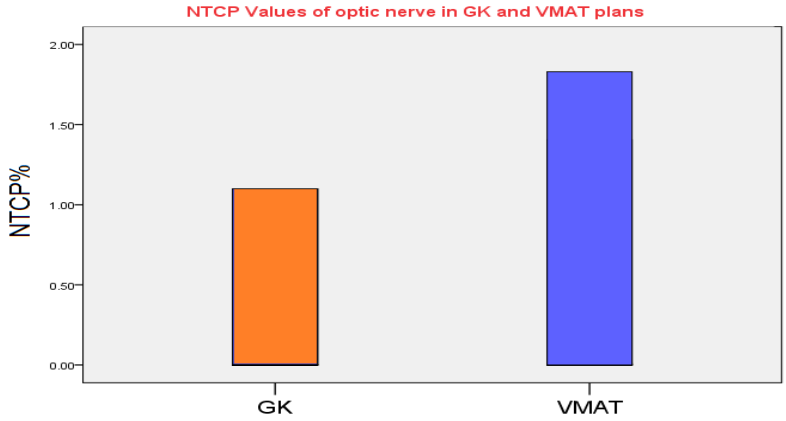

Mean±SD of GK plans 0.00005% ± 0.00008
Mean± SD of VMAT plans 0.0085%± 0.023 ('p'=0.0001, Mann-Whitney test).
Figure 4a. Reveals the effect of the value of NTCP% of the Brain stem for both techniques (GK) and (VMAT) on Meningioma, respectively.

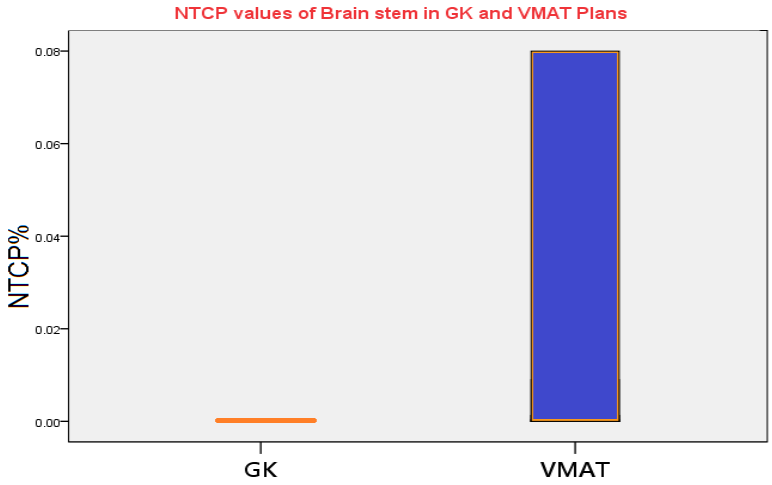

Mean± SD of GK plans 0.13% ± 0.39
Mean± SD of VMAT plans 0.58%± 0.31 ('p'= 0.045, Mann-Whitney test).
Figure 4 b. reveals the effect of the value of NTCP% of optic nerve for both techniques (GK) and (VMAT) on Meningioma, respectively.

The OED and EAR calculations

All OED- and EAR-based outcomes for both planning strategies across the patient cohort are presented in Tables 6 and 7.

Table 6.The mean values of Organ Equivalent dose OED (Mean ± SD) with GK and VMAT Plans for the organs interest for linear, plateau and linear-exponential dose model.

OARs	Model	GK (Mean ± SD)	VMAT (Mean ± SD)	'p'-value
Brain stem	linear	3.18±0.98	4.02±0.17	0.03
	plateau	2.34±0.2	1.12±0.49	0.23
	Linear-exponential	2.4±0.63	2.61±0.13	0.35
Optic nerve	linear	1.41±0.47	1.26±0.55	0.72
	plateau	1.20±0.39	1.12±0.49	0.65
	Linear-exponential	1.27±0.42	1.16±0.51	0.65

Table 7. The excess absolute risk EAR per 10,000 persons per year per Gy (mean ± SD) with GK and VMAT for the organs of interest for Linear, Plateau and Linear-exponential dose- response model.

OARs	Model	GK (Mean ± SD)	VMAT (Mean ± SD)	'p'-value
Brain stem	linear	2.26±0.69	3.95±0.84	0.001
	plateau	1.6±0.54	1.9±0.45	0.3
	Linear-exponential	1.70±0.61	2.3±0.56	0.11
Optic nerve	linear	1.45±0.52	1.19±0.46	0.72
	plateau	0.89±0.93	0.78±0.91	0.93
	Linear-exponential	0.94±0.33	0.81±0.31	0.78

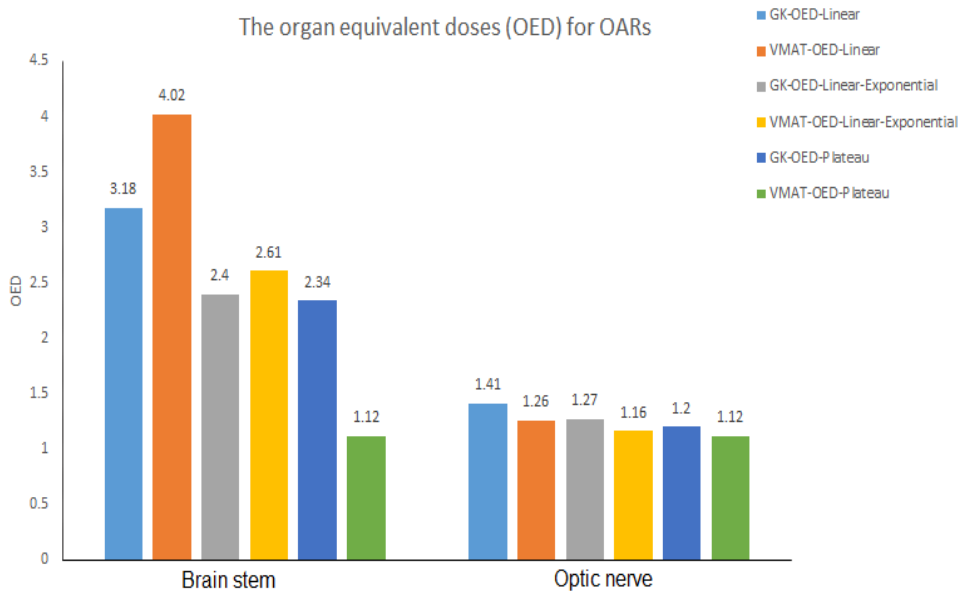

Figure 5. Organ-equivalent dose (OED) values for the evaluated normal tissues (brainstem and optic nerve) were calculated for both GK and VMAT plans using three dose-response models: linear, linear-exponential, and plateau.

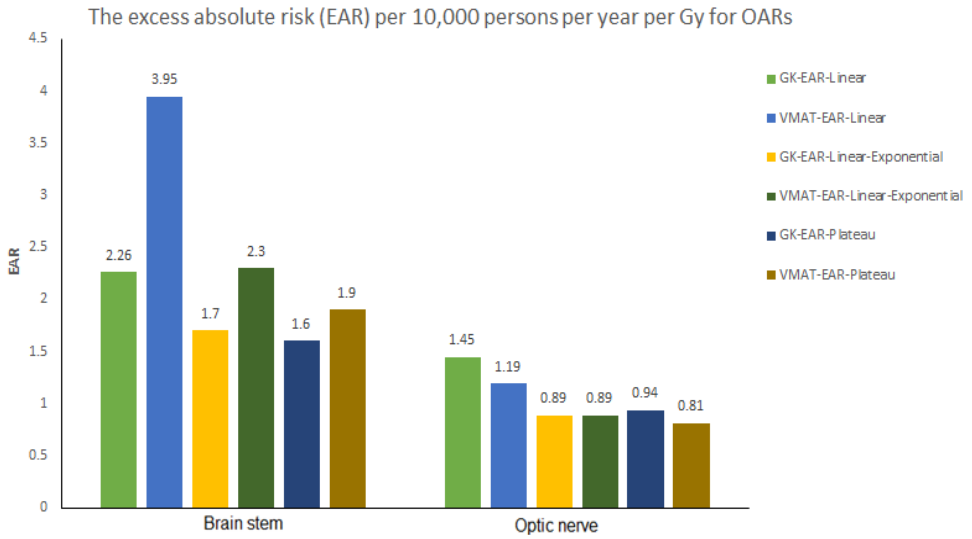

Figure 6. EAR values, expressed per 10,000 persons per year per Gy for the brainstem and optic nerve, were estimated for both GK and VMAT plans using the linear, linear-exponential, and plateau dose–response models.

Table 8.The PTV Mean values of dose-volume parameters comparison for GK and VMAT Plans.

DVH parameters	GK (Mean ±SD)	VMAT (Mean ±SD)	'p'-Value
D95 (%)	12.55±0.23	12±0.0001	0.00012
Dmin(Gy)	8.94±0.93	11.31±0.20	0.00035
Dmax(Gy)	24.22±0.18	13.05±0.25	0.00034
DMean(Gy)	16.81±0.53	12.4±0.13	0.00033
CI	0.97±0.014	0.95±0.016	0.024
HI	2.02±0.016	1.05±0.016	0.00033

Physical and Dosimetric Assessment of Gamma Knife Radiosurgical Plans

All dose–volume parameter results for both planning techniques across the patient cohort are summarized in Table 8.

Table 4 summarizes the EUD and TCP values for meningioma across GK and VMAT plans. Figure 3 illustrates the variation in TCP (%) within the PIV for both techniques. When comparing TCP outcomes, GK planning demonstrated a significantly higher tumor control probability than VMAT (95.76%±2.86 vs. 84.29%± 2.27; 'p'= 2.8×10^{-6}).

Table 5 (a, b) shows EUD as well as NTCP for the Brain Stem and optic nerve in GK and VMAT Plans. Figure 4(a,b) demonstrates the effect of the value of NTCP% of the Brain stem and optic nerve for both techniques (GK) and (VMAT), respectively. Comparing the NTCP of the Brain stem and optic nerve with GK plans to VMAT plans, a statistically significant improvement was observed: 0.00005% ± 0.00008 vs. 0.0085% ± 0.023, 'p'= 0, 0001 and 0.13% ± 0.39 vs. 0.58%± 0.31, 'p'= 0.045, respectively.

Table 6 presents the mean OED values (Mean ± SD) for both GK and VMAT plans for the evaluated organs using the linear, linear-exponential, and plateau dose-response models. Figure 5 graphically depicts the corresponding OED estimates for the brainstem and optic nerve across both techniques under the three radiobiological model assumptions. Comparing the relative OED for the linear model of the Brain stem with GK plans to VMAT plans, a statistically significant improvement was seen (3.18±0.98 vs. 4.02±0.17, 'p'=0.03), whereas a statistically not significant improvement related to plateau and linear-exponential dose–response models 2.34±0.2 vs. 1.12±0.49, 'p'= 0.23, and 2.4±0.63 vs. 2.61±0.13, 'p'= 0.35, respectively.

Table 7 presents the mean EAR values (Mean ± SD), expressed per 10,000 persons per year per Gy, for the brainstem and optic nerve using GK and VMAT plans based on the linear, linear-exponential, and plateau dose-response models. Figure 6 illustrates the corresponding EAR estimates for both techniques across the three modeling approaches. A statistically significant reduction in EAR was observed with GK planning compared with VMAT when applying the linear model for the brainstem (2.26 ± 0.69 vs. 3.95 ± 0.84; 'p' = 0.001). In contrast, differences between GK and VMAT were not statistically significant when evaluated using the plateau model (1.6 ± 0.54 vs. 1.9 ± 0.45; 'p' = 0.30) or the linear-exponential model (1.70 ± 0.61 vs. 2.3 ± 0.56; 'p'= 0.11).

A statistically insignificant improvement was observed in the relative EAR for linear, plateau, as well as linear-exponential dose-response models of the optic nerve with GK plans compared to VMAT plans, respectively. The improvements were 1.45±0.52 vs. 1.19±0.46, 'p'=0.72,

0.89±0.93 vs. 0.78±0.91, 'p'=0.93, and 0.94±0.33 vs. 0.81±0.31, 'p'= 0.78.

The PTV Mean values for the GK and VMAT Plans dose-volume parameter comparison. Mean ± SD of D95 (%) is 12.55±0.23 vs. 12±0.0001, 'p' = 0.00012; Mean ± SD of Dmin, Dmean, and Dmax are 8.94±0.93 vs. 11.31±0.20, 'p'= 0.00035, 16.81±0.53 vs. 12.4±0.13, 'p'= 0.00033, and 24.22±0.1853 vs. 13.05±0.25, 'p'= 0.00034. A statistically significant improvement was exhibited regarding the (Mean ± SD) for the dosimetric parameters.

A statistically significant improvement was observed in the Mean ± SD for CI and HI of PTV using GK plans compared to VMAT plans, with 0.97 ± 0.014 vs. 0.95 ± 0.016, 'p'= 0.024, and 2.02 ± 0.016 vs. 1.05 ± 0.016, 'p'= 0.00033.

Discussion

According to current understanding of ionizing radiation's carcinogenic effects, radiation exposure is likely to be responsible for at least some of these diseases. Stereotactic radiation can significantly reduce local recurrence rates in meningioma patients and boost survival rates. However, radiation can have long-term consequences for healthy tissues in the treated region, such as secondary cancer. To maximize the benefit of radiotherapy for meningioma patients while limiting the risk of radiation-induced secondary cancers, a robust and risk-based evaluation is required.

In this research, treatment protocols for cerebral meningioma involving GK and VMAT were evaluated based on radiobiological results, including TCP and NTCP, alongside target dose-metric indices and OAR dosage characteristics. Additionally, the cancer risk was estimated using EAR calculations obtained from linear, linear-exponential, and plateau dose-response models for both treatment modalities. When comparing dose-coverage metrics for the PTV, GK demonstrated superior performance over VMAT ('p' < 0.05).

CI with GK plans outperformed VMAT plans in the present study by a statistically significant margin (0.97 ± 0.014 vs. 0.95 ± 0.016, 'p'= 0.00033). In GK, the HI has a superior value with VMAT plans, at 1.05±0.016, compared to 2.02±0.016 ('p'= 0.022). According to the study's findings, GK enhanced dose conformity and homogeneity, which improves cosmetic outcomes and reduces the toxicity of late treatment for meningiomas [4-22].

Using the MATLAB-based eudmodel.m platform, the present study evaluated the radiobiological performance of GK and VMAT plans through TCP and NTCP modeling. Incorporation of real patient DVH data enabled quantitative plan assessment and facilitated clinically relevant interpretation for both radiation oncologists and medical physicists. A significantly higher TCP was observed with GK compared with (95.76%±2.86 vs. 84.29%± 2.27; 'p'= 2.8×10^{-6}). These findings are concordant with the results reported by Birckhead et al. [22]., who attributed the excellent tumor control observed with GKRS in NF-2–associated meningiomas to effective dose conformity and the comparatively modest prescription doses used (median 12 Gy; interquartile range 12–14 Gy) [22].

Additionally, the NTCP for the brain stem is higher with GK plans (0.00005% ± 0.00008) than with VMAT (0.0085% ± 0.023; ‘p’ = 0.0001). Additionally, the GK plans for the optic nerve showed a better value (0.13% ± 0.39 vs. 0.58% ± 0.31 in VMAT with 'p'= 0.045). According to the study's findings, GK increased the likelihood of tumor control and reduced normal tissue problems in the brain stem and optic nerve, thereby improving cosmetic outcomes and lowering the risk of late treatment-induced toxicity to the OARs [16].

In the current research, OED values derived from different dose–response models were applied to estimate secondary cancer risk for organs located within both high- and low-dose regions. It is essential to acknowledge that substantial uncertainty exists regarding the true form of the dose–response relationship at therapeutic dose levels exceeding approximately 2 Gy.

At higher radiation doses, the competing influence of radiation-induced cell kill and sterilization of pre-mutated cells becomes increasingly relevant, making linear extrapolation of second cancer risk less reliable. In this study, OED estimates derived from all three dose-response models were significantly greater with GK compared with VMAT, particularly for structures anatomically adjacent to the target, such as the optic nerve. Correspondingly, EAR for the optic nerve increased by 11.23%, 13.17%, and 14.86% using the linear, plateau, and linear-exponential models, respectively, with GK relative to VMAT. In contrast, EAR for the brainstem was higher with VMAT, with relative increases of 54.4%, 17.14%, and 30.0% across the linear, plateau, and linear-exponential models, respectively[24].

Beyond radiotherapy-related exposure, the likelihood of developing a second primary malignancy among cancer survivors may also be influenced by non-treatment factors, including lifestyle behaviors, inherited genetic predisposition, and prior systemic chemotherapy [25]. Epidemiological reports indicate that approximately 17–19% of cancer survivors eventually develop a subsequent malignancy following their initial treatment course [26].

Given the relatively recent and expanding clinical use of GK, robust long-term epidemiological data regarding its potential role in inducing second primary malignancies remain limited. Moreover, published evidence remains inconclusive regarding whether VMAT confers a higher or lower carcinogenic risk compared to GK. In the present analysis, VMAT provided superior PTV dose coverage and dose homogeneity, whereas GK achieved more favorable OAR sparing for the brainstem and optic nerve based on NTCP modeling. However, GK was associated with a relatively higher estimated secondary cancer risk in normal structures, likely attributable to a larger volume of surrounding tissues exposed to low-dose radiation.

The comparison of second cancer risk across the linear, plateau, and linear-exponential response models showed greater divergence at higher OED values, reflecting model sensitivity at elevated dose regions. Conversely, the three models produced more comparable estimates when organ OED values were low, indicating reduced model-dependent variability under low-dose conditions.

This study has some limitations. First, the sample size was limited to 11 patients, which may affect the generalizability of the results. However, the small cohort size reflects the primary objective of the study, which was to compare treatment techniques rather than to investigate inter-patient variability. Second, second cancer risk estimates were derived using dose–response models proposed by Schneider et al. (2011), which, although widely used, carry inherent uncertainties, especially in the high-dose region typical of radiotherapy. Third, the analysis was restricted to a limited number of delineated organs at risk near the tumor. Risk estimates for other brain structures were not assessed due to the lack of contouring and the unavailability of model parameters required for accurate risk computation. Finally, treatment plans were generated using two separate planning systems for Gamma Knife and VMAT, which may introduce uncertainties in dose distribution comparisons and, consequently, in second cancer risk assessment.

Conclusion

Both GKR and VMAT achieved acceptable PTV dose coverage; however, GKR demonstrated superior target coverage, conformity, and dose homogeneity in meningioma planning. GKR also provided better sparing of critical OARs located within high-dose regions, namely the brainstem and optic nerve. Conversely, GKR exposed a larger volume of surrounding normal tissue to low-dose radiation and yielded a higher mean dose to non-target structures compared with VMAT. Evaluation using EAR-based modeling revealed that VMAT resulted in a higher estimated secondary cancer risk compared to GKR. These findings highlight the need for a comprehensive assessment of modern cranial radiotherapy techniques, including dosimetric, radiobiological, and secondary malignancy risk metrics—particularly when treating younger patients with long anticipated survival.

References

1. Ostrom QT, Cioffi G, Gittleman H, Patil N, Waite K, Kruchko C, et al. CBTRUS Statistical Report: Primary Brain and Other Central Nervous System Tumors Diagnosed in the United States in 2012–2016. Neuro Oncol. 2019;21:v1–v100.
2. Brastianos PK, Galanis E, Butowski N, Chan J. W Dunn IF, GoldbrunnerR, et al. Advances in multidisciplinary therapy for meningiomas. Neuro-oncology. 2019; 21(Supplement_1): i18-i31.
3. Rockhill J, Mrugala M, Chamberlain MC. Intracranial meningiomas: an overview of diagnosis and treatment. Neurosurgical focus. 2007; 23(4), E1.
4. Elbaz GY, Hendam HM, Alashkar EM, ABOUELGHEIT HH, Ereiba KM, Attalla EM. (2023). Quality of Radiosurgical Plans by Leksell Gamma Knife Perfexion in the Treatment of Meningioma: Comparison between two isodose lines (50% and 75%). Iranian Journal of Medical Physics. 2023; 20(1): 19-30.
5. Sakthivel V, Mani GK, ManiS, Boopathy R. Radiation-induced second cancer risk from external beam photon radiotherapy for head and neck cancer: impact on in-field and out-of-field organs. Asian Pacific journal of cancer prevention: APJCP. 2017; 18(7): 1897.
6. Lee HF, Lan JH, Chao PJ, Ting HM, Chen HC, Hsu HC, et al. Radiation-induced secondary malignancies for nasopharyngeal carcinoma: a pilot study of patients treated via IMRT or VMAT. Cancer Management and Research. 2018; 10: 131–41.
7. Soliman MI, Attia WM, Elshahat KM. Dosimetric Evaluation Study of 10-MV FFF Used in SBRT for Lung Tumours. East European Journal of Physics. 2023; (3): 457-65.
8. El-Agamawi, Ahmed Yousry, El-Shahat Khaled, ElGharbawy, Esmail Rasmy. Inverse Versus Forward IMRT Planning in Adjuvant Conventional Radiotherapy in Left Breast Cancer in correlation to cardiac constraints (A Retrospective Study). Al-Azhar International Medical Journal. 2024; 5(12): Article24.
9. AB EI. LGP 10 Leksell Gamma Plan®. Online Reference Manual. 2011; 1023200 Rev. 01.
10. Allen Li X, Alber M, Deasy JO, Jackson A, Ken Jee KW, Marks LB, et al. The use and QA of biologically related models for treatment planning: Short report of the TG-166 of the therapy physics committee of the AAPM. Medical physics. 2012; 39(3): 1386-409.
11. Abo-Madyan Y, Aziz MH, Aly MM, Schneider F, Sperk E, Clausen S, et al. Second cancer risk after 3D-CRT, IMRT and VMAT for breast cancer. Radiotherapy and Oncology. 2014; 110(3): 471-6.
12. Zwahlen DR, Ruben JD, Jones P, Gagliardi F, Millar JL, Schneider U. Effect of intensity-modulated pelvic radiotherapy on second cancer risk in the postoperative treatment of endometrial and cervical cancer. International Journal of Radiation Oncology* Biology* Physics. 2009; 74(2): 539-45.
13. Schneider U, Sumila M, Robotka J. Site-specific dose-response relationships for cancer induction from the combined Japanese A-bomb and Hodgkin cohorts for doses relevant to radiotherapy. Theoretical Biology and Medical Modelling. 2011; 8: 1-21.
14. Schneider U, Walsh L. Cancer risk estimates from the combined Japanese A-bomb and Hodgkin cohorts for doses relevant to radiotherapy. Radiation and environmental biophysics. 2008; 47: 253-63.
15. Paddick I, Lippitz B. A simple dose gradient measurement tool to complement the conformity index. Journal of neurosurgery. 2006; 105(Supplement): 194-201.
16. Gay HA, Niemierko A. A free program for calculating EUD-based NTCP and TCP in external

beam radiotherapy. Physica Medica. 2007; 23(3-4): 115-25.
17. Ezz Elregal A, Hussain MS ED, El-Shahat KM. Evaluation of Preoperative Short Course Intensity Modulated Radiation Therapy in Treatment of Locally Advanced Rectal Carcinoma. Al-Azhar International Medical Journal. 2020; 1(8): 74-86.
18. Mansour Z, Attalla EM, Sarhan A, Awad IA, Hamid MI. Study the influence of the number of beams on radiotherapy plans for the hyopfractionated treatment of breast cancer using biological model. J Adv Physics. 2019; 16: 377-90.
19. Gregoire V, Mackie TR. Dose prescription, reporting and recording in intensity-modulated radiation therapy: a digest of the ICRU Report 83. Imaging in Medicine. 2011; 3(3): 367.
20. Langer M, Morrill SS, Lane R. A test of the claim that plan rankings are determined by relative complication and tumor-control probabilities. International Journal of Radiation Oncology* Biology* Physics. 1998; 41(2): 451-7.
21. Moiseenko V, Battista J, Van Dyk J. Normal tissue complication probabilities: dependence on choice of biological model and dose-volume histogram reduction scheme. International Journal of Radiation Oncology* Biology* Physics. 2000; 46(4): 983-93.
22. Birckhead B, Sio TT, Pollock BE, Link MJ, Laack NN. Gamma Knife radiosurgery for neurofibromatosis type 2-associated meningiomas: a 22-year patient series. Journal of neuro-oncology. 2016; 130(3): 553-60.
23. Practical implementation of a collapsed cone convolution algorithm for a radiation treatment planning system. Journal of the Korean Physical Society. 2012; 61: 2073-83.
24. Preston DL, Ron E, Tokuoka S, Funamoto S, Nishi N, Soda M, et al. Solid cancer incidence in atomic bomb survivors: 1958–1998. Radiation research. 2007; 168(1): 1-64.
25. Dracham CB, Shankar A, Madan R. Radiation induced secondary malignancies: a review article. Radiation oncology journal. 2018; 36(2): 85.
26. Morton LM, Onel K, Curtis RE, Hungate EA, Armstrong GT. The rising incidence of second cancers: patterns of occurrence and identification of risk factors for children and adults. In American Society of Clinical Oncology Educational book. American Society of Clinical Oncology. Annual Meeting. 2014; e57-67.
27. Hassan M, Attalla EM. Second cancer risk evaluation from breast radiotherapy using dose-response models. Egyptian Journal of Biomedical Engineering and Biophysics. 2021; 22(1): 29-43.
28. Scoccianti S, Detti B, Gadda D, Greto D, Furfaro I, Meacci F, et al. Organs at risk in the brain and their dose-constraints in adults and in children: a radiation oncologist′s guide for delineation in everyday practice. Radiotherapy and Oncology. 2015; 114(2): 230-8.